DESIGNED ANISOTROPY IN BRITTLE CERAMICS: MICA AS A MODEL SYSTEM

The contents of this chapter are based on work from the journal article "Obreimoff revisited: Controlled heterogeneous fracture through the splitting of mica" by M.T. Johnson, N.R. Brodnik, T. Ekeh, K. Bhattacharya, and K.T. Faber. This article has been accepted to the journal *Mechanics of Materials* and is pending publication.[1] M.T. Johnson and N.R. Brodnik were both listed as first authors on this publication, as they collaborated on both the experimental design as well as the testing of samples and production of figures.

0.1 Introduction

The influence of designed anisotropy on fracture behavior was demonstrated in the previous chapters with brittle polymer systems fabricated using digital light processing. However, these experiments also showed some of the challenges that arise with the transition to fracture in ceramics. Many of these challenges arise from the fact that failure properties are dependent not only on the fracture toughness of a material, but also its stiffness, and the combination of these two properties dictates how well a material can dissipate energy during failure. Many ceramics have fracture toughness values similar to those seen in brittle polymers, but they are thousands of times stiffer, which makes them far worse at dissipating energy during fracture, and this makes controlling and measuring failure response much more challenging.

This control of failure behavior plays a critical role when analyzing heterogeneous ceramic structures centers with discrete crack interaction events. When a heterogeneous structure is being used to influence macroscopic toughness and the structure itself is discrete (cannot be approximated as a single continuous material), the only way that the effect of inclusions can be properly evaluated is if the toughness of the system can be measured before, during, and after crack-inclusion interaction. This greatly constrains the number of available methods for evaluating toughness, as the system must be loaded in a way that provides continuous stable crack growth throughout the entirety of the interaction between crack and inclusion. If stability of the system changes as the crack lengthens, as occurs in tests such as compact tension and bending, the measured toughness will be dependent on the absolute position of the inclusions within the sample, which is not useful for assessment of material properties.[2] As previously demonstrated, surfing load is able to achieve continuous

stable crack growth, but it has limitations regarding the stiffness of materials that can be tested.[2] One test that has been shown to demonstrate global stability, however, is small-angle wedge splitting, which can readily be done on ceramics with layered crystallographic structures.[2]

The earliest forms of small-angle wedge splitting are almost as old as the field of fracture mechanics itself. In 1931, just 10 years after Griffith's work [3], J.W. Obreimoff performed an experiment to investigate whether or not the surface chemistry mechanisms that produced contact bonding were the same mechanisms that governed brittle fracture.[4] In the experiment, muscovite mica, which is known to cleave smoothly along the (001) crystallographic plane, was split with a blunted glass wedge, and the curvature of the split mica surface was used to determine the energy required for separation, which is a combination of the surface energy for the newly formed surfaces 2γ and the mechanical energy required to bend the cleaved mica sheet with the wedge. After the first splitting, the wedge was retracted and the mica was split a second time to determine if the fracture would heal and subsequently re-separate, as is the case with contact bonding of smooth surfaces. The results demonstrated that contact bonding and fracture are fundamentally different, and the latter is not fully reversible. Moreover the fracture energy of mica is dependent on the environment in which it is fractured, as the presence of air, or more specifically water vapor in air, reduces the energy required to form new surfaces.[4] As previously discussed, this is also one of the earliest published fracture studies to demonstrate continuous stable crack propagation [2], which has been established as critical for the understanding of discrete interactions between cracks and heterogeneous structures.

In the time since Obreimoff's study, mica has been a material of research interest both mechanically as well as chemically. Its layered structure creates smooth pathways along which fracture can occur, allowing for controlled observation of brittle fracture where the crack front is constrained to a single plane. Wedge opening experiments similar to Obreimoff's have been used to investigate in greater detail the crack healing abilities of mica as well as the kinetic aspects of thin interface fracture.[5] Additional splitting experiments have been used to study the fracture and contact energies of mica-mica and mica-silica interfaces in moist environments as well as the effects of crack damage recovery and interface misorientation on mica interfaces.[6, 7] Beyond mechanical characterization, pristine cleaved mica surfaces can also be functionalized and used as substrates for thin film growth.[8, 9]

Although wedge splitting presents great promise in terms of achieving stable crack

growth, challenges still arise with the introduction of heterogeneous structure into a naturally layered system like mica. Fortunately, a reliable method for producing heterogeneous structure in constrained fracture has already been established in a related context. Recently, there has been great interest in how contrast in material properties of composite constituents can affect strength and toughness. However, studying and simulating the fracture behavior of composite structures across multiple dimensions and length scales can prove difficult, so these composite systems are often constrained in one or more dimensions. One of simplest methods for applying this type of constraint is tape peeling, where the toughness of the tape system is the work of adhesion originally described by Rivlin [10], and the stiffness is affected by changing either the thickness or material composition of the tape. Traditionally, tape that is being peeled can be described as a membrane, but elasticity plays a role in peeling behavior in cases where the tape is under large tensile stresses or the peeling angle is small.[11] This latter case is of particular interest because when elasticity plays a significant enough role, tape peeling can be a reasonable analog to fracture. Furthermore, a tape peeling with a small peel angle can be seen in several respects to be similar to wedge splitting with a small splitting angle, so techniques for introducing heterogeneous structure should translate well between techniques.

In the case of tape peeling with small peel angles, several studies have demonstrated that either compliance or elastic contrast in tape can produce a significant change in the required peel force without any alteration to the work of adhesion itself.[11–14] This contrast can be produced by either introducing multiple layers of tape to vary stiffness or by changing the polymer composition of the tape substrate without changing the adhesive. Similar behavior has been shown in the constrained fracture of three-dimensional printed specimens with different polymer layers as well as in the separation of glass from soft adhesive substrates, where variations in composition can be used to change both the composition and adhesive properties of the substrate, which would alter the analogous stiffness and toughness respectively.[12, 14–18] Finally, the effect of stiffness and toughness contrast in constrained fracture has also been demonstrated numerically both for tape peeling as well as for fracture of heterogeneous materials.[19, 20]

Tape peeling studies provide promising insight into the fracture mechanics of multi-material composites, but they can only provide limited information about failure of stiff, brittle systems like ceramics, as they typically rely on soft polymeric materials with large cohesion zones and low elastic moduli, which ultimately affect

the resultant failure behavior.[21] This is where the layered structure of muscovite mica presents a promising opportunity for the investigation of brittle fracture. Small angle wedge splitting of mica can provide constrained, continuously stable, brittle fracture of a model system with high stiffness, where heterogeneous structure can be readily introduced. First, homogeneous muscovite mica is split with a glass wedge similar to Obreimoff's experiments to establish a baseline material behavior. Once homogeneous material behavior is established, thickness variations are introduced into the system to study how compliance contrast affects both the required splitting force as well as the subsequent failure behavior in ceramics. Finally, the implications of this investigation are then discussed in the context of the design of layered ceramic composites.

0.2 Methods

0.2.1 Materials

Mica samples for testing were prepared from sheets (V-1 quality, Electron Microscopy Sciences, Hatfield, PA, USA) designed for atomic force microscope applications. Individual mica sheets, nominally 25 x 75 x 0.26-0.31 mm^3, were burnished lightly on 400 grit paper to remove edge defects that may have been introduced in prior cutting operations. Sheet dimensions were unchanged from processing, and care was taken to prevent any visible mica cleavage during handling. For testing, individual samples were mounted vertically on a T-shaped aluminum sample holder using wafer mounting adhesive (Wafer-Mount 559, Electron Microscopy Sciences) following Figure 0.1a.

0.2.2 Mechanical Testing

In the context of this study, the force required to split the mica was used as an indirect analog to the measurement of actual fracture toughness, which requires measurement of the curvature of the mica. Although measuring the splitting force is indirect, it should still be a good predictor of the toughness of the system so long as the system is quasi-static and the wedge is advanced slow enough to allow the fracture front to equilibrate with each propagation event. The quartz wedge used to apply this splitting force was prepared from a quartz sheet (150 x 50 x 1 mm^3) polished to a 25° angle using abrasive paper. This polished edge was flame-treated to remove any residual polishing marks and gently round the tip of the wedge. The prepared wedge was mounted in an Instron 5982 mechanical testing frame (Instron Corporation, Norwood, MA) and aligned vertically with the angled tip oriented away from the

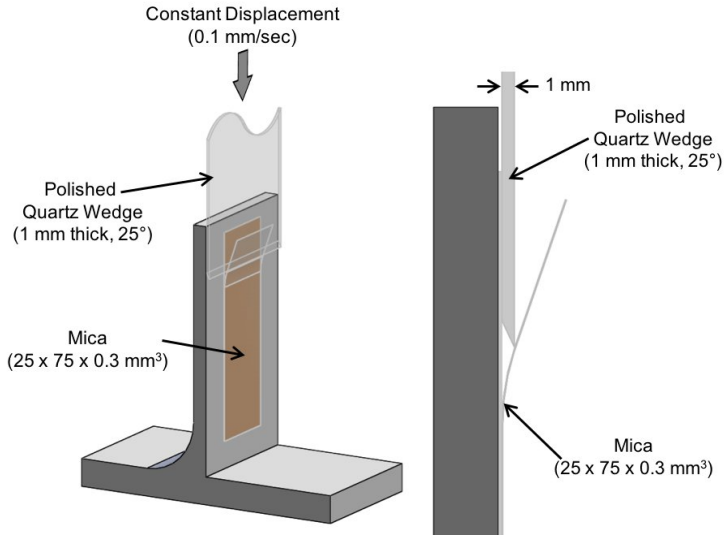

(a) Testing Schematic (b) Testing Profile

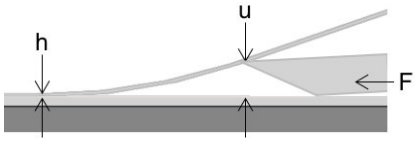

(c) Testing Profile, detail

Figure 0.1: Schematics showing (a) the mica splitting sample setup, (b) a side profile of the cleavage front, and (c) the wedge orientation in more detail.

mica sample following Figure 0.1b. This orientation was chosen to encourage the wedge to smoothly pass over any defects or height variations present in the substrate mica, which reduces the occurrence of both undesired pinning of the wedge as well as tearing of the cleaved sheet during testing. In all testing, the mica cleavage front extends a considerable distance (5 to 20 mm, depending on cleaved sheet thickness) in front of the wedge.

An initial cleavage crack was started by hand using a razor blade prior to insertion of the quartz wedge for testing. Tests were performed with a constant displacement rate of 0.1 mm*s^{-1} until the cleavage crack extended fully through the sample. Samples demonstrating an abundance of defects — typically in the form of tearing or pinning from edge defects — were discarded. To monitor crack propagation, still images were taken at five second intervals through the duration of testing. A mirror was used to simultaneously capture both the face and profile of samples, and images were synchronized to force-displacement curves to correlate propagation events with measured mechanical response.

0.2.2.1 Homogeneous Samples

A initial series of 27 mica samples with homogeneous cleave layer thickness, shown schematically in Figure 0.2, were tested in order to validate test methods and determine a correlation between measured splitting force and the thickness of the cleaved mica layer. Mica sheets of thicknesses ranging from 0.01 to 0.16 mm were cleaved from larger mounted samples. The measured force was averaged over the steady-state portion of the test to determine the splitting force for a given sample. Typically, the first 10-15 mm of test displacement as well as the last 15-20 mm were discarded from averaging, as these regions tended to show edge effects either from the initiation of the crack with a razor or from the cleave front approaching the end of the sample. Within the measurement region, samples sometimes showed the presence of transient increases in load above the steady-state, which were fully recoverable. Due to their random nature, these events occurred at varying locations in the measurement region and their prevalence tended to increase with increasing thickness. Samples with sufficiently few of these events to still achieve a steady-state condition were included in analysis, with the events themselves removed from averaging.

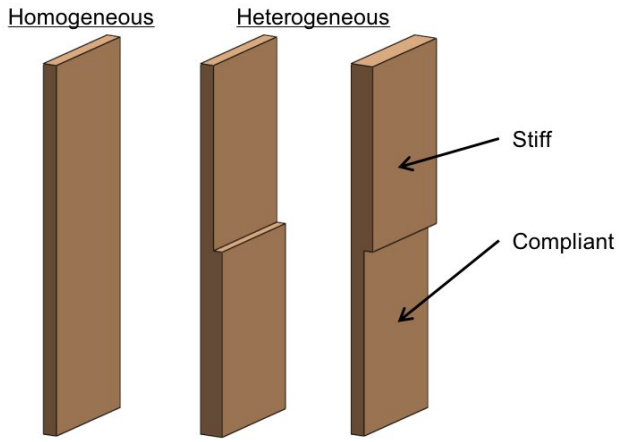

Figure 0.2: Schematic of homogeneous and heterogeneous sample profiles.

0.2.2.2 Heterogeneous Samples

A second series of samples were prepared with prescribed thickness variations to alter the bending stiffness in different regions along the length of the fracture plane as shown in Figure 0.2. A razor blade and straight edge were used to hand-scribe a parting line near the middle of the sample, which marks the location of the heterogeneity. Mica sheets above or below this parting line were cleaved by hand to create a step-wise thickness transition. After splitting of heterogeneous specimens,

the thicknesses of the two different sections of the cleaved sheet were measured, and the difference in thickness between these sections was taken to be the overall height of the heterogeneity.

0.3 Results and Discussion

0.3.1 Homogeneous Samples

A variety of different homogeneous mica sheet thicknesses were tested both to build a baseline of expected splitting forces as well as to determine the intrinsic toughness of the mica, which is directly related to the surface energy of the basal cleavage planes in the mica crystal. Establishing this baseline is particularly critical for later heterogeneous studies because mica's stiffness of 200 GPa [2] is much higher than the polymers used tapes or other soft substrates, so the elastic component of the separation energy is significantly larger than in the case of heterogeneous tape peeling or other membrane separation.

Load-displacement curves for a representative selection of mica cleavage thicknesses are shown in Figure 0.3. These curves each show an initial increasing load regime over approximately the first 10 mm of displacement as well as an observable load drop within the final 10-15 mm of displacement, both of which are likely due to edge effects. Between these loading and unloading sections exists a generally constant splitting load that scales proportionally with the thicknesses of the cleaved mica sheet. Of note in the 0.04 mm, and more notably in the 0.06 mm curves, transitory increases in force are evident in the 20-30 mm and 50-60 mm displacement ranges respectively. These increases in force are due to localized imperfections such as edge defects or localized sheet tears. These effects were characterized by their random occurrence and magnitude, and in some cases, small local tears could even be visually observed. There was no strong indicator to the occurrence of these imperfections, but they tended to be more prevalent in the splitting of thicker sections of mica. As previously mentioned, these defect events, as well as initial loading and unloading periods, were omitted when calculating the mean splitting force. Observations of samples following testing showed that, with the exception of small local tears, cleavage propagation was dictated by the layered structure of mica, with splitting events never deviating from the initial cleavage plane regardless of the thickness or structure of the cleaved sheet.

Originally described by Obreimoff[4] in terms of surface energy, γ, and later by Williams[22] using energy release rate, G, the width-normalized force, F/b, can be

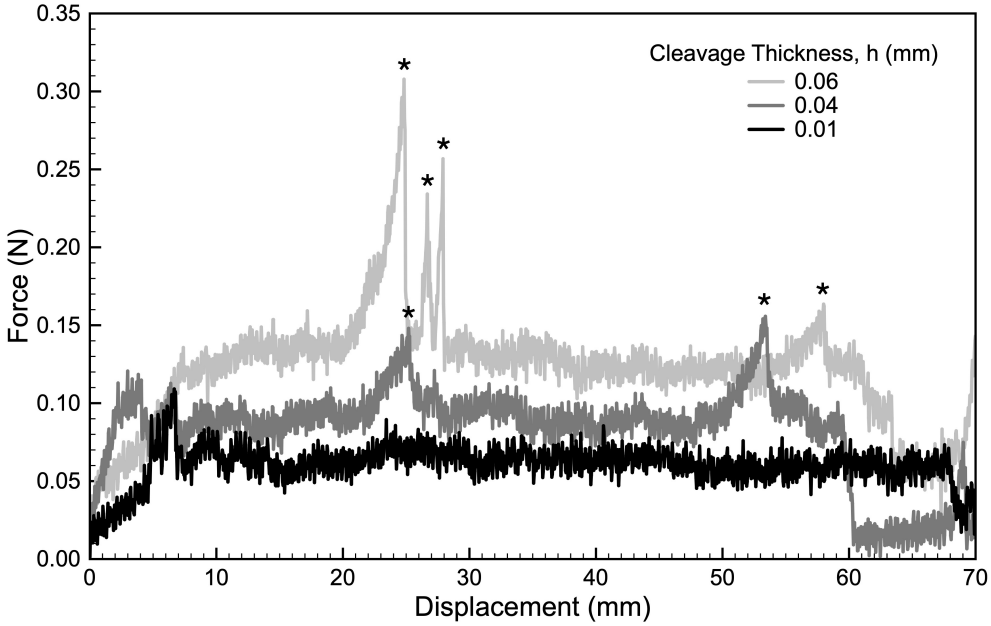

Figure 0.3: Load vs. displacement for the cleavage of select homogeneous mica layers. Transitory increases in force (*) due to edge defects or localized tears were excluded from analysis.

correlated to cleavage thickness, h, following

$$\frac{F}{b} \approx G\left(1 + \frac{\mu}{\alpha}\right) \tag{1}$$

where α is a geometric factor related to the angle of contact between the wedge face and the mica sheet that can be described as

$$\alpha = 3\left(\frac{u}{h}\right)^{\frac{1}{2}}\left(\frac{G}{6Eh}\right)^{\frac{1}{4}} \tag{2}$$

where u is wedge thickness, E is elastic modulus, and μ is the coefficient of friction between wedge and mica. These relations, developed by Williams for the case of small angles, account for elastic deformations, but omit plastic deformation. Friction is also accounted for in the mathematical expression, but quantifying friction experimentally is not straightforward, so some variability is expected in this regard. The assumptions of elastic deformation and small splitting angles are considered to be appropriate though, as no permanent deformations were observed in cleaved mica sheets and the crack tip extends approximately 10 mm in advance of the wedge face, so the largest angles of deflection achieved are of the order of 20°, which is within the range for which the small angle assumption used by Williams is valid.[22]

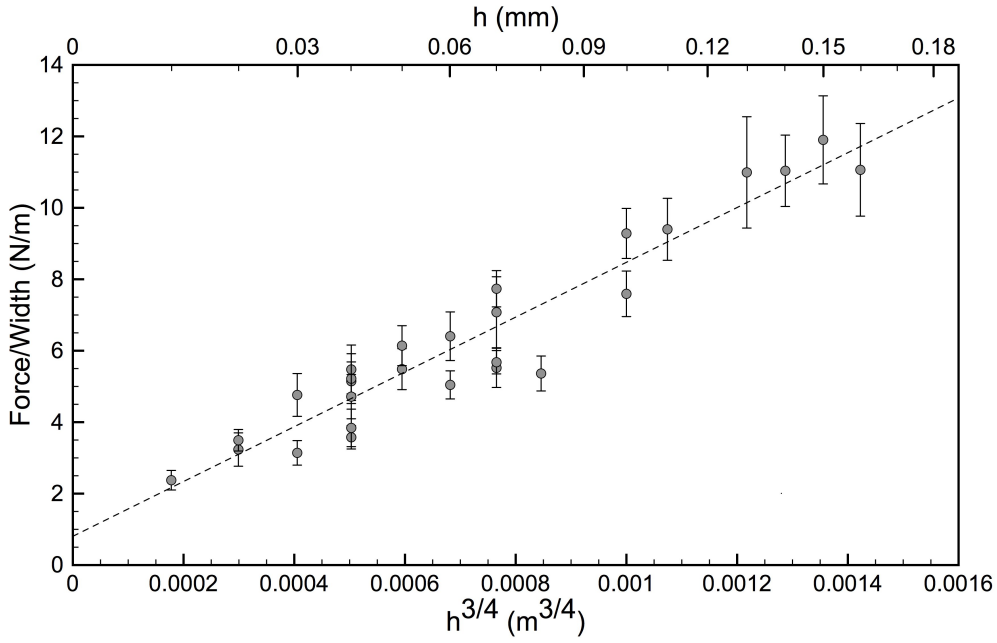

Figure 0.4: Width-normalized average force vs cleavage thickness, $h^{\frac{3}{4}}$.

Shown in Figure 0.4, a regression of normalized force with respect to $h^{\frac{3}{4}}$ reveals a linear trend which corresponds well to Equation 1. The intercept of this regression line is a measure of the normalized force associated with cleaving an infinitely thin mica sheet, which can otherwise be seen as energy required for the creation of two new mica surfaces or the thickness independent critical strain energy release rate, G_c. The critical strain energy release rate in air was measured in this work to be $0.81 \pm 0.38 \frac{J}{m^2}$. Obreimoff's original G_c, determined via surface-energy analysis and expressed as 2γ, was determined to be $0.76 \frac{J}{m^2}$.[2, 4] Similarly, Wan et al. measured mica-mica adhesion energy across a range of relative humidities; they observed energies in the range of 0.6 to 0.8 $\frac{J}{m^2}$ at humidities of 20% and above.[7]

Much of the variability in splitting strength seen in this study is likely due to the combination of frictional effects and natural variations in mica. However, with sufficient replicates across a range of thicknesses, this variation can be accounted for, and a G_c value can be determined that is in good agreement with those found in literature. This agreement indicates that the wedge cleavage techniques developed here are appropriate for the measurement of splitting strengths for the range of mica thicknesses examined in this study.

0.3.2 Heterogeneous Samples

Mica samples with thickness heterogeneities were prepared and tested in an analogous fashion to samples of homogeneous thickness. Shown in Figure 0.5 are two loading curves for mica samples of 0.03 mm initial thickness and 0.06 mm final thickness with a step-wise change of thickness at approximately 30 mm of displacement. Both of these samples show similar loading behavior to their homogeneous analogs, whose range of splitting strengths (with uncertainties included) are shown in the shaded regions. Additionally, the observed loads in the constant-thickness regions before and after the step-wise thickness change are in good agreement with predicted load values based upon Equation 1 and Figure 0.4. However, unique to samples of heterogeneous thickness is the significant increase in force as the crack interacts with the sudden change in mica thickness. Like the homogeneous samples discussed earlier, there was no observed change in crack path at any point during testing as the crack stayed fully constrained to the cleavage plane. The observed increase in splitting force, approximately 5x above the baseline, combined with no change to the crack path indicates that the presence of an increased-thickness heterogeneity has increased the effective macroscopic toughness of the mica system well over that of homogeneous structures of equivalent thickness. These observations are not explained by the classical analyses of Obreimoff and Williams, where only constant-thickness cleavage is addressed.

As the cleavage front passes from compliant (thin) regions to stiff (thick) regions, the front experiences a rapid change in stored elastic energy within the portion of the mica sheet that is being bent. As the crack front interacts with the thickness increase, the work being done by the advancing wedge transfers from propagating the crack to bending the split mica layer, slowing crack advancement. The geometry of the wedge splitting setup makes it difficult to precisely predict the splitting force enhancement due to this change in thickness, as all sources of friction as well as the exact wedge thickness and exact sheet thickness need to be known, and this is not straightforward. However, a good analytical indicator of the expected splitting force enhancement is the differences in flexural rigidity between the two regions of the heterogeneous mica sheet. This approach has been used to describe similar contrast in membrane peeling. Based on this, the splitting force enhancement can be estimated as

$$\frac{F_{heterogenous}}{F_{homogeneous}} = \frac{D_{stiff}}{D_{compliant}} \tag{3}$$

where D is the bending rigidity, which is described as

$$D = \frac{Ebh^3}{12\left(1-\nu^2\right)} \tag{4}$$

where E is elastic the modulus, b is the width of the mica sheet, b is the thickness of the cleaved layer in the region being evaluated, and ν is Poisson's ratio. It follows from this that for the case of heterogeneous mica, the change in splitting force is proportional to h^3 for a bending beam, so changes in splitting force should scale with the cubed magnitude of the change in thickness across the heterogeneity. For the mica dimensions in Figure 0.5 this would predict an eight-fold enhancement in cleavage force, though again, some variation is expected due to differences in test geometry between membrane peeling and wedge splitting. Xia et al. did observe an eight-fold peeling force enhancement in experiments on polyester-backed adhesive tape on epoxy substrates, but these were more precisely analogous to direct peeling of membranes.[12]

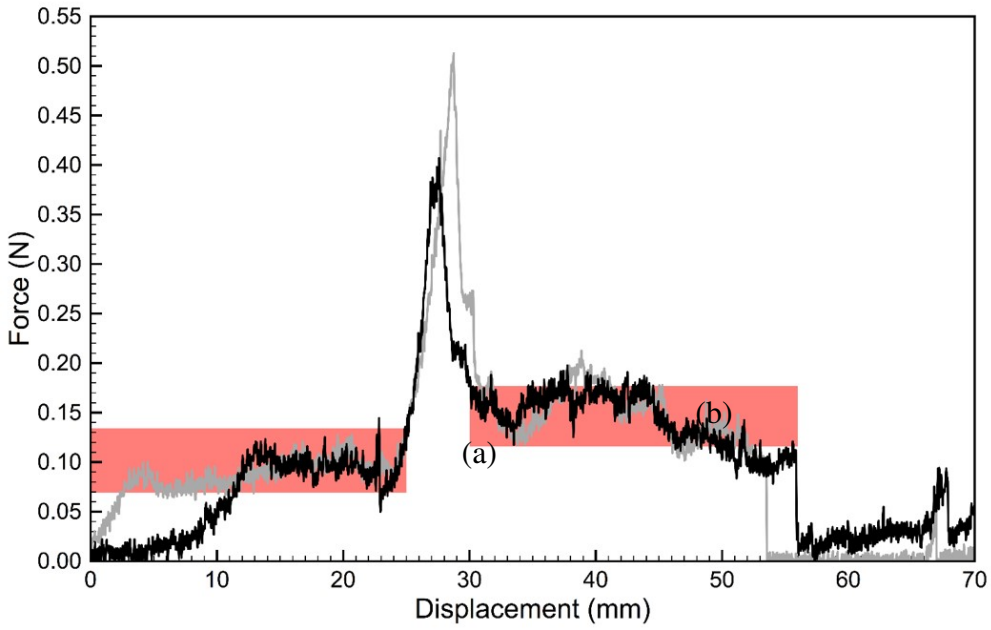

Figure 0.5: Load vs. displacement for the cleavage of mica layers with thickness heterogeneities. Heterogeneities took the form of step-wise thickness increases, from 0.03 to 0.06 mm, at approximately 30 mm of displacement. The shaded region (a) corresponds to the force required to split a homogeneous sheet of thickness 0.03 mm and the shaded region (b) corresponds to the force required to split a homogeneous sheet of thickness 0.06 mm.

To visually correlate crack position to force enhancement, Figure 0.6 shows a

progression of still profile images correlated to specific positions in the load-displacement curve for a 0.03 to 0.06 mm thickness change. Figure 0.6A shows the crack position well in advance of the quartz wedge at the approximate moment where the crack meets the thickness step as indicated by the dotted line across each photo. Figure 0.6B shows a growing increase in curvature of the separated mica layer while the cleavage front appears to still be pinned by the step-wise change of thickness. Figures 0.6C and D show continuing increases in curvature as the splitting force reaches its maximum value. After the thickness step, Figure 0.6E shows a return to behavior similar to the homogeneous splitting conditions where the crack front has become unpinned and has jumped forward, reducing the curvature of the cleaved mica layer.

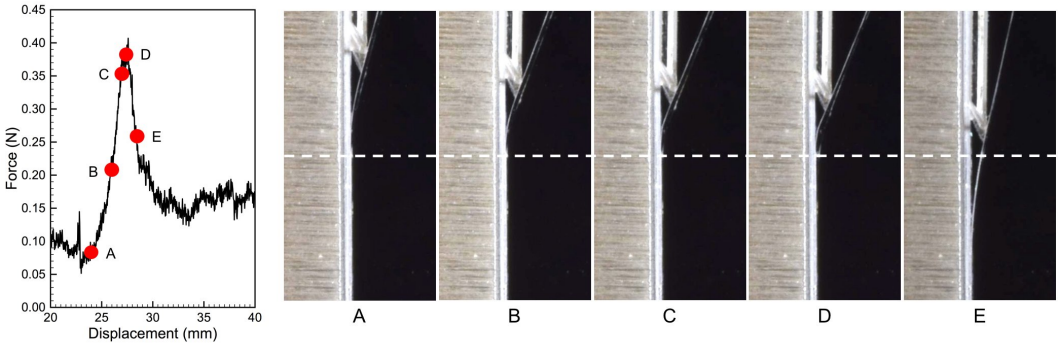

Figure 0.6: Profile still image progression of cleavage crack interacting with a 0.03 to 0.06 mm step-wise thickness change. Image labels correlate to points indicated in Force v. Displacement plot.

Figure 0.7 shows orthogonal face-on views of the same loading stills shown in Figure 0.6. Solid blue lines indicate the position of the advancing quartz wedge while the light gray shading tracks the furthest progress of the crack front. The general position of the crack tip in this perspective correlates well to the profile view; however, some curvature of the crack front is evident immediately after the thickness heterogeneity. As the load builds, Figure 0.7A and B, the crack front stays stationary at the thickness step. Near the point of peak load, Figure 0.7C and D, the crack front has migrated past the heterogeneity on the left-hand side of the mica sheet while still being pinned on the right-hand side. After passing the thickness step, Figure 0.7E, the crack front has jumped further ahead of the quartz wedge as the influence of the heterogeneity is passed.

Unlike in previous tape-peeling and soft membrane studies, where the peeling front propagates past the thickness heterogeneity coupled with an instantaneous drop in

peel force, the cleavage force in these tests falls more gradually, over the span of approximately 5 mm of displacement. This delayed load drop correlates well to the time delay associated with the crack passing the thickness heterogeneity, as illustrated in the progression in Fig 0.7. Likewise, the eight-fold enhancement of cleavage force as predicted by bending rigidity is likely not fully realized since the the cleavage front propagates through the heterogeneity unevenly across the width of the specimen. This could be due to a number of effects including natural variations in the mica as well as slightly imperfect orientation of the wedge with respect to the thickness heterogeneity. This imperfect orientation arises because the wedge is flame polished to minimize surface roughness and reduce the occurrence of unwanted pinning. Although the flame polish was done with great care, it is difficult to obtain a perfectly parallel wedge front, and because the wedge front dictates the equilibrium crack position, this would correlate to a crack front that is not perfectly parallel to the thickness heterogeneity. This deviation from parallel would cause the energy buildup to be slightly uneven along the crack front at the heterogeneity, which may have contributed to both the spread in the measured load increase as well as the fact that the peak load increase was only a factor of 5 over the homogeneous case rather than the factor of 8 predicted by membrane separation models.

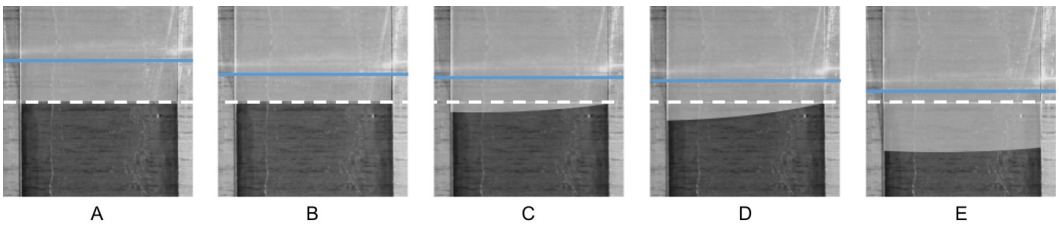

Figure 0.7: Face-view still image progression of a top-to-bottom cleavage crack interacting with a 0.03 to 0.06 mm step-wise thickness change. Images correlate to load-displacement curve positions shown in Figure 0.6. The horizontal solid blue line indicates quartz wedge position, light gray shading (enhanced for clarity) indicates the extent of the cleavage crack, and the thickness step is marked by the white dashed line.

Considering the opposite case of a decreasing thickness heterogeneity, Figure 0.8 shows the loading curve for a mica sample prepared with a step-wise thickness decrease from 0.04 to 0.01 mm. Before and after the thickness change at approximately 30 mm of displacement, the load profile remains consistent with samples of similar homogeneous thickness. Significant differences, however, are evident as the cleavage front interacts with the decrease in sample thickness. A load drop, at approximately 24 mm of displacement, occurs as the crack tip, extending ahead of the quartz wedge,

passes from relatively stiff (thick) to complaint (thin) regions. The cleavage force recovers to a plateau correlating to the predicted value for a 0.01 mm thickness after a brief transition region. The abrupt decrease in splitting force is consistent with the sudden change in compliance that would make crack propagation more favorable. However, the transition region after the jump is believed to be an artifact of the cleavage front propagating well in advance of the wedge tip; although the cleavage front has passed to the thinner region, the thickness step has yet to pass the wedge tip, which is moving at a fixed velocity. Therefore, the change in bending rigidity, which is dictated by the location of the wedge, occurs slightly later than the crack entering the thinned mica. It should be noted that the drop in strength seen in this transition region does not follow the h^3 scaling predicted by differences in flexural rigidity, but this expected because the sudden forward movement of the crack well beyond tip of the wedge indicates a deviation from the ideal equilibrium, so the analytical assessment will not necessarily be a good predictor. Regardless, an enhancement of cleavage force is not realized in this case because the transition from a stiffer material to a softer one actually allows the crack to propagate more readily rather than pinning it.

0.3.3 Implications for Layered Composite Materials

The increase in required force for separation along a cleavage plane in heterogeneous mica is particularly noteworthy because it shows that compliance contrast, or more explicitly a sharp increase in bending stiffness, near the crack tip can affect the force required to propagate a crack, which will manifest as a higher splitting strength. This effect of both elastic and compliance contrast on toughness have been demonstrated in various forms in softer systems, but in this study, a clear confirmation is made in a brittle system with a small cohesive zone and small splitting angles. This makes the study a promising analog to illustrate how compliance contrast or stiffness contrast could improve macroscopic toughness in brittle ceramics with layered structures.

Many layered ceramic structures rely on interfaces to deflect cracks and dissipate energy, but previous studies have also demonstrated the potential of layered ceramics with strongly bonded interfaces which could greatly benefit from the toughness gained through elastic modulus contrast. These strongly bonded, layered ceramic structures are typically composed of a hard thin brittle outer layer and a much thicker functional layer beneath that is typically more compliant and damage tolerant. These types of layered structures have been shown to be beneficial in bilayer composites, which are useful in applications such as thermal barrier coatings and dental implants,

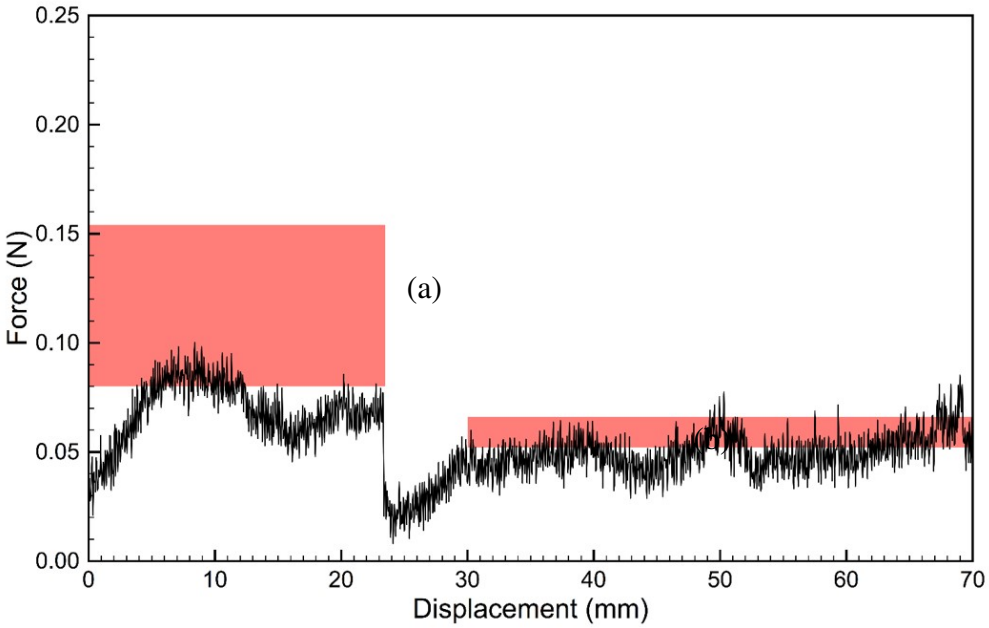

Figure 0.8: Load vs. displacement for the cleavage of mica with a thickness heterogeneity. The heterogeneity took the form of step-wise thickness decrease, from 0.04 to 0.01 mm, at approximately 30 mm of displacement. The shaded region (a) corresponds to the force required to split a homogeneous sheet of thickness 0.04 mm and the shaded region (b) corresponds to the force required to split a homogeneous sheet of thickness 0.01 mm.

where resistance to impact and indentation are critical.[23–31] However, functional layers often rely on defects and small cracks to accommodate deformations, and concerns can arise in cases where the functional layer develops cracks that are sufficiently large that it can no longer effectively accommodate mechanical loads without failing catastrophically.[23, 32] In these scenarios, the results of this study indicate that the addition of internal hard brittle layers, either as a complete layer or fractions of layers, may be of significant benefit in limiting the propagation of larger cracks in the functional layer through the presence of significant elastic contrast. If the elastic contrast is sufficiently large, the presence of these additional internal layers could increase the toughness of the composite well above the toughness of its constituent components. Furthermore, the spacing of these hard brittle layers could be adjusted to tailor the functionality of the layered composite to sufficiently resist indentation damage as well as limit the propagation of larger internal cracks. This additional toughening through elastic contrast at strong interfaces presents interesting opportunities for toughening in layered ceramic composites that are, to date, not well

investigated.

0.3.4 Implications for Designed Asymmetry

In the context of designed anisotropy, muscovite mica with added thickness variations also demonstrates how heterogeneous structure can be used to create directionally-dependent macroscopic fracture properties. Based on analytical assessments of membrane separation, the peak wedge splitting force measured across a thickness heterogeneity scales with the cube of the magnitude of the thickness difference in the ideal case. But even with deviations from ideality, the scaling is still some exponential of the height difference that is larger than 1. This nonlinear scaling is important because if macroscopic fracture toughness is considered to scale with the maximum splitting force, then a heterogeneous mica specimen with two separate 0.3 mm thickness increases should exhibit lower macroscopic toughness than a specimen with one 0.6 mm thickness increase. This same argument could also be applied in reverse to the compliance changes associated with a decreases in thickness. Logical extension of this leads to the argument that the macroscopic toughness anisotropy of the mica sheet could be maximized by introducing a large thickness increase followed by many small, consecutive thickness decreases. This design would maximize the peak splitting force and minimize the subsequent load drop in one direction, while minimizing peak force and maximizing load drop in the other direction, all while keeping the crack constrained to stable, continuous growth in a single fracture plane.

Attempts were made to demonstrate this directional anisotropy within one mica sheet in a single experiment, but it proved infeasible, as uniform mica sheets of sufficient length could not be produced, so it was not possible to achieve steady state propagation after each heterogeneity and get accurate measurements of splitting strength. Attempts were made to achieve this effect in larger sheets of natural mica (Ward's Science, Rochester, NY) rather than sectioned sheets for atomic force microscopy (V-1 quality, Electron Microscopy Sciences, Hatfield, PA, USA), but these natural sheets had too many natural defects and pinning sites to be suitable for fracture study. Finally, a similar exploration of this topic was done in the context numerical simulations of idealized heterogeneous media with equivalent toughnesses and different stiffnesses.[19] Similar multi-material studies may also be possible in the context of mica by filling in thickness variations with a resin or other soft phase, but steps must be taken to prevent the second phase from infiltrating over the top of or between mica layers. However, even without the addition of a second phase, these experiments on muscovite mica readily demonstrate that compliance

contrast can directly improve both the strength and toughness of a brittle composite structure as well as introduce toughness anisotropy that is dependent on the direction of propagation of the crack within a singular orientation.

0.4 Summary

Following an experimental procedure inspired by Obreimoff, muscovite mica specimens were separated along cleavage planes under displacement controlled conditions using a polished quartz wedge. The force required for separation was measured, and related to the critical energy release rate, a combination of the surface energy and elastic bending energy of the cleaved mica sheet. Homogeneous mica separation was performed for a variety of sheet thicknesses to establish the baseline thickness dependence. These observations were then applied to investigate the behavior of heterogeneous mica sheets with designed, step-wise thickness heterogeneities.

In mica prepared with thickness heterogeneities, a dramatic increase in required separation force occurred when the mica splitting front encountered the thickness increase in the mica sheet. This force enhancement is associated with a change in flexural rigidity of the cleaved mica sheet, and the increase in force observed is significantly larger than the splitting force required for the homogeneous constituents.

The results of this study indicate that compliance contrast near the tip of a crack can dramatically alter the magnitude of the required driving force to propagate a crack, which will manifest as an increase in macroscopic fracture toughness. This phenomenon could prove to be of significant benefit in layered ceramic composites with strongly bonded interfaces where more compliant layers are used beneath high-stiffness brittle layers to absorb damage from impact and indentation. This study suggests that the incorporation of additional high-stiffness layers may serve to mitigate crack growth and improve failure strength. Additionally, these studies of heterogeneous structures in mica demonstrate the potential for macrosopic improvements of toughness in ceramic composites through the introduction of elastic contrast or compliance contrast. This same elastic and compliance contrast can also be used to introduce toughness properties that are dependent on the direction of crack propagation.

REFERENCES

[1] M.T. Johnson, N.R. Brodnik, T. Ekeh, K. Bhattacharya, and K.T. Faber. Obreimoff revisited: Controlled heterogeneous fracture through the splitting of mica. *Mechanics of Materials*, 136:103088, sep 2019. ISSN 0167-6636. doi: 10.1016/J.MECHMAT.2019.103088. URL https://www.sciencedirect.com/science/article/pii/S0167663618307543?dgcid=author.

[2] Brian R. Lawn. *Fracture of brittle solids*. Cambridge University Press, 1993. ISBN 9780511623127.

[3] A. A. Griffith. The Phenomena of Rupture and Flow in Solids. *Philosophical Transactions of the Royal Society A: Mathematical, Physical and Engineering Sciences*, 221(582-593):163–198, jan 1921. ISSN 1364-503X. doi: 10.1098/rsta.1921.0006. URL http://rsta.royalsocietypublishing.org/cgi/doi/10.1098/rsta.1921.0006.

[4] J. W. Obreimoff. The Splitting Strength of Mica. *Proceedings of the Royal Society of London A*, 25:290–297, 1930. ISSN 1364-5021. doi: 10.1098/rspa.1933.0074.

[5] Lawn B. R. Roach, D. H., Hueckeroth, D. M. Crack Velocity Thresholds and Healing in Mica. *Journal of Colloid and Interface Science*, 114(1):292–294, 1986.

[6] Kai-tak Wan, Nicholas Aimard, S Lathabai, Roger G Horn, and Brian R. Lawn. Interfacial energy states of moisture-exposed cracks in mica. *Journal of Materials Research*, 5(1):172–182, 1990. ISSN 08842914. doi: 10.1557/JMR.1990.0172.

[7] Kai-Tak Wan, Douglas T. Smith, and Brain R. Lawn. Fracture and Contact Adhesion Energies of Mica-Mica, Silica-Silica, and Mica-Silica Interfaces in Dry and Moist Atmospheres. *Journal of the American Ceramic Society*, 75 (3):667–676, mar 1992. ISSN 0002-7820. doi: 10.1111/j.1151-2916.1992.tb07857.x. URL http://doi.wiley.com/10.1111/j.1151-2916.1992.tb07857.x.

[8] Hiroshi Okusa, Kazue Kurihara, and Toyoki Kunitake. Chemical Modification of Molecularly Smooth Mica Surface and Protein Attachment. Technical report, 1994. URL https://pubs.acs.org/sharingguidelines.

[9] Hong Yang, Alex Kuperman, Neil Coombs, Suzan Mamiche-Afara, and Geoffrey A. Ozin. Synthesis of oriented films of mesoporous silica on mica. *Nature*, 379(6567):703–705, feb 1996. ISSN 0028-0836. doi: 10.1038/379703a0. URL http://www.nature.com/articles/379703a0.

[10] Rivlin R. S. The Effective work of adhesion Experiments with Adhesive Tape. *Paint Technology*, IX(106):2611–2614, 1944.

[11] K Kendall. Thin-film peeling-the elastic term. *Journal of Physics D: Applied Physics*, 8(13):1449–1452, sep 1975. ISSN 0022-3727. doi: 10.1088/0022-3727/8/13/005. URL http://stacks.iop.org/0022-3727/8/i=13/a=005?key=crossref.1fe0609b9b564ad02f86ea972699bc29.

[12] S. Xia, L. Ponson, G. Ravichandran, and K. Bhattacharya. Toughening and Asymmetry in Peeling of Heterogeneous Adhesives. *Physical Review Letters*, 108(19):1–5, may 2012. ISSN 0031-9007. doi: 10.1103/PhysRevLett.108.196101. URL https://link.aps.org/doi/10.1103/PhysRevLett.108.196101.

[13] S.M. Xia, L. Ponson, G. Ravichandran, and K. Bhattacharya. Adhesion of heterogeneous thin films—I: Elastic heterogeneity. *Journal of the Mechanics and Physics of Solids*, 61(3):838–851, mar 2013. ISSN 0022-5096. doi: 10.1016/J.JMPS.2012.10.014. URL https://www.sciencedirect.com/science/article/pii/S0022509612002359.

[14] S.M. Xia, L. Ponson, G. Ravichandran, and K. Bhattacharya. Adhesion of heterogeneous thin films II: Adhesive heterogeneity. *Journal of the Mechanics and Physics of Solids*, 83:88–103, oct 2015. ISSN 0022-5096. doi: 10.1016/J.JMPS.2015.06.010. URL https://www.sciencedirect.com/science/article/pii/S0022509615001593.

[15] A Majumder, S Mondal, A K Tiwari, A Ghatak, and A Sharma. Direction specific adhesion induced by subsurface liquid filled microchannels. *Soft Matter*, 8(27):7228–7233, 2012. ISSN 1744683X (ISSN). doi: 10.1039/c2sm25507c. URL http://www.scopus.com/inward/record.url?eid=2-s2.0-84869594034{\&}partnerID=40{\&}md5=ff1ba1eafe4330c24c1a2f4598ac51d8.

[16] Animangsu Ghatak. Peeling off an adhesive layer with spatially varying topography and shear modulus. *Physical Review E - Statistical, Nonlinear, and Soft Matter Physics*, 89(3):1–6, 2014. ISSN 15502376. doi: 10.1103/PhysRevE.89.032407.

[17] J. Gonzalez and J. Lambros. Crack Path Selection in Microstructurally Tailored Inhomogeneous Polymers. *Experimental Mechanics*, 53(4):619–634, apr 2013. ISSN 0014-4851. doi: 10.1007/s11340-012-9668-3. URL http://link.springer.com/10.1007/s11340-012-9668-3.

[18] Neng Wang and Shuman Xia. Cohesive fracture of elastically heterogeneous materials: An integrative modeling and experimental study. *Journal of the Mechanics and Physics of Solids*, 98:87–105, jan 2017. ISSN 0022-5096. doi: 10.1016/J.JMPS.2016.09.004. URL https://www.sciencedirect.com/science/article/pii/S0022509616303313.

[19] M. Z. Hossain, C. J. Hsueh, B. Bourdin, and K. Bhattacharya. Effective toughness of heterogeneous media. *Journal of the Mechanics and Physics of Solids*, 71(1):15–32, 2014. ISSN 00225096. doi: 10.1016/j.jmps.2014.06.002. URL http://dx.doi.org/10.1016/j.jmps.2014.06.002.

[20] C-J. Hsueh, L. Avellar, B. Bourdin, G. Ravichandran, and K. Bhattacharya. Stress fluctuation, crack renucleation and toughening in layered materials. *Journal of the Mechanics and Physics of Solids*, 120:68–78, nov 2018. ISSN 0022-5096. doi: 10.1016/J.JMPS.2018.04.011. URL https://www.sciencedirect.com/science/article/pii/S0022509617311407.

[21] C. Kovalchick, A. Molinari, and G. Ravichandran. An experimental investigation of the stability of peeling for adhesive tapes. *Mechanics of Materials*, 66: 69–78, nov 2013. ISSN 0167-6636. doi: 10.1016/J.MECHMAT.2013.07.012. URL https://www.sciencedirect.com/science/article/pii/S0167663613001415.

[22] J. G. Williams. Friction and plasticity effects in wedge splitting and cutting fracture tests. *Journal of Materials Science*, 33(22):5351–5357, November 1998. ISSN 1573-4803. doi: 10.1023/A:1004490015211. URL https://doi.org/10.1023/A:1004490015211.

[23] Brian R. Lawn. Indentation of Ceramics with Spheres: A Century after Hertz. *Journal of the American Ceramic Society*, 81(8):1977–1994, jan 1998. ISSN 00027820. doi: 10.1111/j.1151-2916.1998.tb02580.x. URL http://doi.wiley.com/10.1111/j.1151-2916.1998.tb02580.x.

[24] Haiyan Liu, Brian R. Lawn, and Stephen M. Hsu. Hertzian Contact Response of Tailored Silicon Nitride Multilayers. *Journal of the American Ceramic Society*, 79(4):1009–1014, apr 1996. ISSN 0002-7820. doi: 10.1111/j.1151-2916.1996.tb08540.x. URL http://doi.wiley.com/10.1111/j.1151-2916.1996.tb08540.x.

[25] Antonia Pajares, Lanhua Wei, Brian R. Lawn, and Christopher C. Berndt. Contact Damage in Plasma-Sprayed Alumina-Based Coatings. *Journal of the American Ceramic Society*, 79(7):1907–1914, jul 1996. ISSN 0002-7820. doi: 10.1111/j.1151-2916.1996.tb08012.x. URL http://doi.wiley.com/10.1111/j.1151-2916.1996.tb08012.x.

[26] Antonia Pajares, Lanhua Wei, Brian R. Lawn, Nitin P. Padture, and Christopher C. Berndt. Mechanical characterization of plasma sprayed ceramic coatings on metal substrates by contact testing. *Materials Science and Engineering: A*, 208(2):158–165, apr 1996. ISSN 0921-5093. doi: 10.1016/0921-5093(95)10071-7. URL https://www.sciencedirect.com/science/article/pii/0921509395100717.

[27] A C Fischer-Cripps, B R Lawn, A Pajares, and L Wei. Stress Analysis of Elastic-Plastic Contact Damage in Ceramic Coatings on Metal Substrates.

Journal of the American Ceramic Society, 79(10):2619–2625, aug 1996. ISSN 00027820. doi: 10.1111/j.1151-2916.1996.tb09024.x. URL http://dx.doi.org/10.1111/j.1151-2916.1996.tb09024.x.

[28] Linan An, Helen M. Chan, Nitin P. Padture, and Brian R. Lawn. Damage-resistant alumina-based layer composites. *Journal of Materials Research*, 11(01):204–210, jan 1996. ISSN 0884-2914. doi: 10.1557/JMR.1996.0025. URL http://www.journals.cambridge.org/abstract{_}S0884291400022214.

[29] Donald M. Baskin, Michael H. Zimmerman, K. T. Faber, and Edwin R. Fuller. Forming Single-Phase Laminates via the Gelcasting Technique. *Journal of the American Ceramic Society*, 80(11):2929–2932, nov 1997. ISSN 0002-7820. doi: 10.1111/j.1151-2916.1997.tb03213.x. URL http://doi.wiley.com/10.1111/j.1151-2916.1997.tb03213.x.

[30] Sataporn Wuttiphan, Antonia Pajares, Brian R. Lawn, and Christopher C. Berndt. Effect of substrate and bond coat on contact damage in zirconia-based plasma-sprayed coatings. *Thin Solid Films*, 293(1-2):251–260, jan 1997. ISSN 0040-6090. doi: 10.1016/S0040-6090(96)08992-4. URL https://www.sciencedirect.com/science/article/pii/S0040609096089924.

[31] John K. Montgomery and K. T. Faber. Processing and Surface Flaw Tolerance of Alumina Bilayers. *Journal of the American Ceramic Society*, 88(2):287–292, feb 2005. ISSN 0002-7820. doi: 10.1111/j.1551-2916.2005.00073.x. URL http://doi.wiley.com/10.1111/j.1551-2916.2005.00073.x.

[32] Sataporn Wuttiphan, Brian R. Lawn, and Nitin P. Padture. Crack Suppression in Strongly Bonded Homogeneous/Heterogeneous Laminates: A Study on Glass/Glass-Ceramic Bilayers. *Journal of the American Ceramic Society*, 79 (3):634–640, apr 1996. ISSN 00027820. doi: 10.1111/j.1151-2916.1996.tb07922.x. URL http://doi.wiley.com/10.1111/j.1151-2916.1996.tb07922.x.